ROYAL SOCIETY OF CHEMISTRY

ROYAL SOCIETY OF CHEMISTRY

www.rsc.org/methods

Sensitive and simple detection of trace hydrogen peroxide based on a resonance light scattering assay

Ningli Tang*, Yaqi Shan, Ronghui Zhang, Xinglong Meng

Abstract

In weakly acidic conditions, with haemoglobin (Hb) as a mimetic peroxidase, the oxidizing reaction between H_2O_2 and KI was catalysed by haemoglobin to form I_2, which combined with excessive I^- to form I_3^-. I_3^- then reacted with gold nanoparticles (AuNPs) to produce AuI_2^-, which decreased the resonance light scattering intensity of the gold nanoparticles at 575 nm. The resonance light scattering (RLS) intensity linearly decreased as the hydrogen peroxide concentration increased. On this basis, a new method for the resonance light scattering determination of hydrogen peroxide has been developed, and the optimum reaction conditions, influential factors and application were investigated. Under the optimal reaction conditions, hydrogen peroxide concentrations of $3.25 \times 10^{-7} \sim 2.60 \times 10^{-5}$ mol·L^{-1} were linearly correlated to the reduction in the resonance light scattering intensity (ΔI) with a correlation coefficient of 0.9992 and a detection limit of 2.48×10^{-7} mol·L^{-1}. The new method has been applied to the analysis of hydrogen peroxide in milk samples with satisfactory results.

Keywords: Hydrogen peroxide, Gold nanoparticles, Haemoglobin, Resonance light scattering

1. Introduction

Due to quantum size effects, their small size, surface effects and macroscopic quantum effects, nanoparticles exhibit properties, such as optical, electronic and catalytic performance, that are different from those of macroscopic bulk materials. The size and shape of gold nanoparticles strongly influence their performance. In addition, a morphological change in gold nanoparticles can result in changes in its optical signal because the gold nanoparticles have a high specific surface energy and a negatively charged surface. When a photon is near, it reacts with the interface electronics of gold nanoparticles. Therefore, gold nanoparticles have a wide range of applications in drug testing, genetic testing, immunoassays, and determinations of biomolecular properties [1, 2].

Hydrogen peroxide is both closely related to human health and an essential mediator in food, pharmaceutical, clinical, industrial and environmental analyses [3]. Long-term contact with hydrogen peroxide can decolour human hair and cause respiratory symptoms. However, hydrogen peroxide is an important factor in acid rain because air and rainwater contain H_2O_2. Therefore, the determination of trace amounts of H_2O_2 is very important, and numerous methods have been developed to detect H_2O_2, including electrochemistry (EC) [4-7], titrimetry [8], atomic absorption spectrometry (AAS) [9], high performance liquid chromatography (HPLC) [10,11], chemiluminescence (CL) [12,13], flow-injection analysis (FIA) [14,15], fluorescence spectrometry (FS) [16-18], nuclear magnetic resonance (NMR) [19,20], spectrophotometry [21,22] and resonance light scattering assays (RLS) [23,24]. Resonance light scattering (RLS) is a sensitive and simple analytical technique that has been applied to the analysis of metal ions, proteins, nucleic acids and enzymatic activity [25]. However, the H_2O_2-Hb-KI-AuNPs catalytic system has not been investigated using RLS.

Horseradish peroxidase (HRP) is the most commonly used enzyme in H_2O_2 detection. However,

3

HRP has some disadvantages, such as being expensive and unstable in solution, with harsh reaction requirements and conservation conditions. Therefore, the development of a HRP replacement is needed. Haemoglobin (Hb) is responsible for carrying oxygen. Hb has a natural quaternary structure that consists of four polypeptide subunits, and each subunit contains a haem as the active centre. Recent studies determined that Hb has oxidant activities and can be used as a mimetic of HRP and that the catalytic activity of Hb is much higher than that of haemin and some metalloporphyrins because Hb has a natural quaternary structure. Hb exhibits several advantages for the determination of H_2O_2 compared to the commonly used catalysts due to its high activity and low cost (Hb is 150 times less expensive than HRP). However, to the best of our knowledge, the application of Hb as peroxidase mimetic for the RLS analysis of H_2O_2 has not yet been reported.

In this study, for the first time, an unmodified gold nanoparticle based resonance light scattering method for H_2O_2 detection was developed using Hb and KI as the catalyst and substrate, respectively. In principle, the oxidizing reaction between H_2O_2 and KI was catalysed by Hb to form I_2, which combined with excessive I^- to form I_3^-. According to the theory of iodine leaching of gold, I_3^- reacted with the AuNPs to produce AuI_2^-, resulting in smaller gold nanoparticles, and the resonance light scattering intensity of the system decreased. The analysis conditions have been optimized, and the performance of the proposed system was investigated. Several distinct advantages, such as simplicity, low cost and high sensitivity, make this approach a potentially useful tool for H_2O_2 detection.

2. Experimental

2.1. Reagents and solutions

Bovine haemoglobin, chloroauric acid ($HAuCl_4·4H_2O$) and trichloracetic acid (TCA) were purchased from Sinopharm Chemical Reagent Co. Ltd. (Shanghai, China). Hydrogen peroxide (30%,

w/v solution) was purchased from Shantou Xilong Chemical Co. Ltd. (Guangdong, China), and the

H_2O_2 concentration (4.04×10^{-2} mol·L^{-1}) in the stock solution was standardized by titration with

potassium permanganate. Potassium iodide was purchased from Shanghai Qiangshun Chemical

Reagent Co. Ltd. (Shanghai, China). A 1.0% (w/v) trisodium citrate solution was prepared. A 0.01

mol·L^{-1} HAc-NaAc buffer solution (pH 4.5-5.9), 0.01 mol·L^{-1} citric acid-trisodium citrate buffer

solution (pH 4.5-5.9) and Clark-Lub's (C-L) buffer solution (pH 4.5-5.9) were also prepared. All of the

materials and reagents were used as received, and all of the solutions were prepared with ultrapure

water.

2.2 Apparatus

The RLS spectra were measured with a RF-5301 spectrofluorometer (Shimadzu, Japan) by

synchronously scanning the excitation wavelength (λex) and emission wavelength (λem;

λex$-\lambda$em=$\Delta\lambda$=0). UV-vis spectra were recorded on a Cary 50 spectrophotometer (Varian, America).

Transmission electron microscopy (TEM) was performed on a JEM-2100F field emission transmission

electron microscope (JEOL, Japan). The AuNPs were prepared using a IKA RET digital controlled

magnetic stirring hotplate (IKA, Germany).

2.3 Gold nanoparticle preparation

Gold nanoparticles with an average diameter of 16 nm were prepared by citrate reduction of

$HAuCl_4$ according to the method described in Ref. [26, 27] and its corresponding references. All of the

glassware used in the following procedures was thoroughly cleaned with freshly prepared aqua regia

(three parts HCl and one part HNO_3), washed with ultrapure water, and dried prior to use. First, 1.0 mL

of 1.0% chloroauric acid was added to the 100 mL quartz sub-boiling water, and the boiling was

maintained for 5 min. Then, 6.0 mL of a 1.0% trisodium citrate solution was quickly added to this

solution under vigorous stirring at 1000 rpm and boiled for 15 min. Finally, the heating was terminated,

but the stirring was maintained for 15 min. The nanoparticle solution was left to cool to room

temperature and diluted to 100 mL with quartz sub-boiling water. The concentration of gold

nanoparticles was 58.0 µg/mL. This material was stored in a refrigerator at 4 °C.

2.4 Sample preparation

Two different liquid milk samples (Mengniu and Yili) were commercially obtained from a local

supermarket in Guilin, China. Prior to the determination, 20 mL of 20% (w/v) TCA was added to 20

mL of milk followed by centrifuged at 4000 rpm for 40 min, and the supernatant was further filtered

with a 0.2 µm filter. Then, the H_2O_2 concentration in the filtrate was determined.

2.5 Detection of H_2O_2

First, 0.2 mL of a pH 5.5 citrate buffer solution, 0.3 mL of 0.1 mol·L^{-1} KI, 0.4 mL of $6.2×10^{-6}$

mol·L^{-1} Hb and an appropriate volume of $1.62×10^{-4}$ mol·L^{-1} H_2O_2 were successively added to a 5 mL

marked test tube, and the mixture was diluted to 3 mL with ultrapure water and mixed thoroughly. Next,

the resulting solution was allowed to stand for 20 min at 25 °C. Then, 0.5 mL of a 58.0 µg/mL gold

nanoparticle solution was added, and the mixture was diluted to 5 mL and mixed well. The RLS

intensity at 575 nm (I) was recorded. A blank (I_0) without H_2O_2 was measured, and the value of $\Delta I=I_0$ -

I was calculated.

3. Results and discussion

3.1 Resonance light scattering spectra

The resonance light scattering spectra of the different systems are shown in Fig. 1. The scattering

signal of the citric acid-trisodium citrate buffer solution, KI, Hb and gold nanoparticle systems was

very strong (Fig. 1a). A strong resonance scattering peak was observed at 575 nm. When a certain

amount of H_2O_2 was added to the citric acid-trisodium citrate-KI-Hb-AuNPs system, a catalytic

oxidation reaction occurred rapidly, and the resonance light scattering intensity at 575 nm decreased as

the H_2O_2 concentration increased (Figs. 1c-e). Therefore, 575 nm was selected for use in this assay. As

shown in Figs. 1b and 1c, Hb acted as a catalyst in this system.

Fig. 1

3.2 UV–vis spectra

　　The colour of the mixture consisting of the gold nanoparticle solution and the enzymatic reaction

solution containing KI, Hb and H_2O_2 changed from red to yellow. However, no detectable colour

change was observed after the gold nanoparticles were added to the mixture consisting of KI and Hb

(reagent blank). The corresponding absorption spectra of the mixtures are shown in Fig. 2. The

absorption spectra of the system (Fig. 2a) indicated that Hb exhibited a molecular absorption peak at

405 nm [28]. In addition, the gold nanoparticles exhibited an absorption peak at 575 nm. Upon addition

of H_2O_2, the intensity of the absorption peak corresponding to the gold nanoparticles decreased

substantially (Fig. 2b). In the presence of excess H_2O_2, two new absorption peaks located at 288 nm

and 350 nm were observed in Fig. 2c, which corresponded to the molecular absorption peaks of I_3^-, and

the absorption peak corresponding to the gold nanoparticles nearly disappeared because the gold

nanoparticles were nearly depleted.

Fig. 2

7

3.3 Transmission electron microscopy (TEM)

The TEM images (Fig. 3) indicated that the gold nanoparticles were spherical with a mean diameter of approximately 16 nm in the pH 5.5 citric acid-trisodium citrate buffer solution (Fig. 3a). Upon addition of KI and Hb, the gold nanoparticles aggregated into large clusters of 225 nm in size (Fig. 3b). However, upon addition of H_2O_2, the aggregation effect decreased significantly, and the size decreased to 70 nm (Fig. 3c).

Fig. 3

3.4 Mechanism

In summary, we can propose the following mechanism. In the pH 5.5 citric acid-trisodium citrate buffer solution, I^- was adsorbed onto the gold nanoparticle surface via an oxidation etching reaction to form AuI, which led to the aggregation of the gold nanoparticles. Therefore, the resonance light scattering intensity of the system increased. When H_2O_2 was added, the oxidizing reaction between H_2O_2 and KI was catalysed by Hb to form I_2, which combined with excess I^- to yield I_3^-. According to the theory of iodine leaching of gold [29, 30], I_3^- reacted with the AuNPs to produce AuI_2^- [31], resulting in smaller gold nanoparticles, and the resonance light scattering intensity of the system decreased. The mechanism for the reaction primarily involves the following steps:

Scheme 1

3.5 Effect of the buffer solution

The enzyme active part commonly contains an acidic group and a basic group, and the catalytic

reaction is very sensitive to pH in a narrow range. As the pH varies, these groups are in different

dissociation states, and the activity of Hb changes. Therefore, Hb has an optimal pH. The influence of

three types of buffer solutions (pH 4.5-5.9), including HAc-NaAc, citric acid-trisodium citrate, and C-L,

on the ΔI was investigated. The results in Fig. 4 indicate that the sensitivity decreased in the order of

citric acid-trisodium citrate, C-L and HAc-NaAc. The citric acid-trisodium citrate buffer solution was

most sensitive and stable, and this solution was chosen for use. As described in a previous report [27],

the fresh-synthesized AuNPs solution was deep red, while at low pH values, the AuNPs solution was

dark blue, which might ascribed to the aggregation of AuNPs. The maximum change in the resonance

light scattering intensity was observed at pH 5.5 (Fig. 4). The citric acid-trisodium citrate buffer

solution was the most sensitive and stable, which might ascribed to trisodium citrate solution being the

reductive agent for the preparation of gold nanoparticles. Therefore, a pH 5.5 citric acid-trisodium

citrate buffer solution was chosen for use. The effect of the buffer solution concentration on the ΔI was

investigated. The results indicate that the ΔI value was highest when the concentration of the citric

acid-trisodium citrate buffer solution was 4×10^{-3} mol·L^{-1} (Fig. 5). Therefore, a 4×10^{-3} mol·L^{-1} pH 5.5

citric acid-trisodium citrate buffer solution was chosen for use.

Fig. 4

Fig. 5

3.6 Effect of KI

As the concentration of KI increased (Fig. 6), the ΔI value first increased and then remained

nearly constant. The KI concentration was 6.0×10^{-3} mol·L^{-1} when the reduction of the RLS intensity of

the system peaked. This is because I_3^- was not totally formed when the concentration of KI was below

6.0×10^{-3} mol·L^{-1}. When the concentration of KI reached this value or I$^-$ was added in excess, I_2 reacted

with I$^-$ totally. Thus, the reduction of the RLS intensity of the system peaked and then remained almost

constant. Therefore, a KI concentration of 6.0×10^{-3} mol·L^{-1} was chosen for use.

Fig. 6

3.7 Effect of Hb

Hb was a catalyst in the reaction. The assay cost can be decreased by using a small amount of Hb.

The effect of the Hb concentration on the ΔI value was investigated. As shown in Fig. 7, the Hb

concentration was 4.96×10^{-7} mol·L^{-1} when the reduction of the RLS intensity of the system peaked.

Without Hb as catalyst, the main reaction barely proceeded. Hb concentrations below 4.96×10^{-7} mol·L^{-1}

were not sufficient to decrease the activation energy of the reaction. This Hb concentration

corresponded to the lowest activation energy of the reaction. When Hb was added in excess, it hindered

the main reaction; thus, the reduction of the RLS intensity began to decrease as the Hb concentration

increased beyond 4.96×10^{-7} mol·L^{-1}. Therefore, 4.96×10^{-7} mol·L^{-1} was chosen as the appropriate

concentration of Hb.

Fig. 7

3.8 Effect of the gold nanoparticles

The effect of the gold nanoparticle concentration on the ΔI value was investigated. The results (Fig.

8) indicated that the AuNPs concentration was 5.80 μg·mL^{-1} when the reduction of the RLS intensity of

the system peaked. This is because I$_3^-$ was not totally chelated when the concentration of AuNPs was

below 5.80 μg·mL^{-1}. When the concentration of AuNPs reached this value, I$_3^-$ reacted with AuNPs

totally. When AuNPs were added in excess, unreacted AuNPs aggregated with I$^-$; thus, the reduction of

the RLS intensity began to decrease when the concentration of AuNPs exceeded 5.80 μg·mL^{-1}.

Therefore, 5.80 μg·mL^{-1} was chosen as the appropriate concentration of AuNPs.

Fig. 8

3.9 Effect of the catalytic reaction temperature and time

Under the previously determined conditions of acidity and reagent concentrations, the catalytic

reaction occurred at room temperature (25 °C), which reduced the loss of enzyme activity and avoided

the decomposition of H$_2$O$_2$ at high temperatures. Furthermore, this methodology provides convenient

operation. When the concentration of H$_2$O$_2$ was 6.48×10^{-6} mol·L^{-1}, the effect of the enzyme catalytic

reaction time on the system was determined by measuring the absorbance of I$_3^-$, which was generated in

the first step of the reaction, at 288 nm. The results indicated that the ΔA_{288nm} value reached a

maximum when a 20 min reaction time was employed, and the system was stable by this time.

Therefore, 20 min was selected for use.

3.10 Stability of the system

At room temperature, the stability of the system was tested after the gold nanoparticles were added,

and the results indicated that the ΔI value was stable for 0~30 min. Therefore, the determination can be

performed immediately after the gold nanoparticles are added.

3.11 Calibration curve

Under the optimal conditions, the ΔI values for different H_2O_2 concentrations (C) were determined (Fig. 9). The ΔI value is proportional to the C in the range of $3.25\times10^{-7}\sim2.60\times10^{-5}$ mol·L^{-1}. The regression equation was $\Delta I = 1.280\times10^7$ C + 6.220 with a correlation coefficient of 0.9992 and a detection limit (DL) of 2.48×10^{-7} mol·L^{-1} H_2O_2. The DL was calculated according to the following equation: DL = $3S_b/K$, where 3 is the factor at the 95% confidence level, S_b is the standard deviation of the blank measurements (n = 11), and K is the slope of the calibration curve. In comparison to results from previously reported assays [7, 11, 14, 19, 21, 23, 28] (Table 1), this Hb catalytic RLS method is sensitive and selective as well as rapid and cheap.

Fig. 9

Table 1

3.12 Influence of foreign substances

The influence of coexistence substances on the determination of 6.48×10^{-6} mol·L^{-1} H_2O_2 was investigated according to the previously mentioned procedure with a relative error of ±5.0%. The results are summarized in Table 2. The coexistence of foreign substances did not interfere with the determination of H_2O_2, which demonstrates that the method exhibits good selectivity.

Table 2

3.13 Sample determination

The newly proposed method has been used to determine the amount of H_2O_2 in two milk samples,

and the results are listed in Table 3. In these two milk samples, H_2O_2 was not detected. When 6.48×10^{-6}

$mol \cdot L^{-1}$ and 1.296×10^{-5} $mol \cdot L^{-1}$ H_2O_2 were added to the milk samples respectively, the H_2O_2 recoveries

were in the range of 92.3%-100.3%. The relative standard deviation (RSD) was less than 4.1%. These

results indicated that the new method was satisfactory for practical application to the determination of

H_2O_2.

Table 3

4. Conclusions

A resonance light scattering method has been developed for the determination of trace amounts of

H_2O_2 based on the enzyme catalytic effect of Hb and gold nanoparticle aggregation. Its linear range is

from 3.25×10^{-7} $mol \cdot L^{-1}$ to 2.60×10^{-5} $mol \cdot L^{-1}$ with a detection limit of 2.48×10^{-7} $mol \cdot L^{-1}$ H_2O_2. This

method was applied to determine H_2O_2 in milk samples with satisfactory results.

Acknowledgements

References

[1] C. Jing, F.J. Rawson, H. Zhou, X. Shi, W.H. Li, D.W. Li and Y.T. Long, Anal Chem, 2014, **86**, 5513.

[2]   M.A. O'Connell, J.R. Lewis and A.J. Wain. Chem Comm, 2015, **51**, 10314.

[3] H.C. Guo, H. Aleyasin, B.C. Dickinson, R.E. Haskew-Layton and R.R. Ratan, Cell Biosci, 2014, **4**, 64.

[4] Y.M. Sun, K. He, Z.F. Zhang, A.J. Zhou and H.W. Duan, Biosens Bioelectron, 2015, **68**, 358.

[5] Y.F. Gong, X. Chen, Y.L. Lu and W.S. Yang, Biosens Bioelectron, 2015, 66, 392.

[6]   J. Ju and W. Chen, Anal Chem, 2015, 87, 1903.

[7]   S.Y. Guo, L. Xu, B.B. Xu, Z.X. Sun and L.H. Wang, Analyst, 2015, 140, 820.

[8] C.E. Huckaba and F.G. Keyes, J Am Chem Soc, 1948, 70, 1640.

[9]   Z.L. Jiang, Y.F. Tang, A.H. Liang and Q. Gong, Spectrosc Spect Anal, 2009, 29, 1990.

[10] S.M. Steinberg, Environ Monit Assess, 2013, 185, 3749.

[11] M. Tarvin, B. McCord, K. Mount and M.L. Miller, J Chromatogr A, 2010, 1217, 7564.

[12] J.L. Liu, L.L. Lu, A.Q. Li, J.Tang, S.G. Wang, S.Y. Xu and L.Y. Wang, Biosens Bioelectron, 2015, 68, 204.

[13] A. Tahirovic, A. Copra, E. Omanovic-Miklicanin and K. Kalcher, Talanta, 2007, 72, 1378.

[14] H .Chen, L. Lin, Z. Lin, C. Lu, G. Guo and J.M. Lin, Analyst, 2011, 136, 1957.

[15] R.A. Franchini, M.A. Matos, R. Colombara and R.C. Matos, Talanta, 2008, 75, 301.

[16] N.A. Burmistrova, R.J. Meier, S. Schreml and A. Duerkop, Sensor Actuat B-Chem,2014, 193, 799.

[17] D.H. He, C.B. Zheng, Q. Wang, C.L. He, Y. Li, L. Wu and X.D. Hou, Talanta, 2015, 142, 51.

[18] H.Q. Chen, H.P. Yu, Y.Y. Zhou and L. Wang, Spectrochim. Acta Part A, 2007, 67, 683.

[19] N. Stephenson and A. Bell, Anal Bioanal Chem, 2005, 381, 1289.

[20] C. Tsiafoulis and I. Gerothanassis, Anal Bioanal Chem, 2014, 406, 3371.

[21] N. Wang, J.C. Sun, L.J. Chen, H. Fan and S.Y. Ai, Microchim Acta, 2015, 182, 1733.

[22] Q. Zhang, S.Y. Fu, H.L. Li and Y. Liu, BioResources, 2013, 8, 3699.

[23] H.X. Ouyang, S.W. Huang and Z.L. Jiang, Bull Chem Soc Ethiop, 2011, 25, 161.

[24] G.Q. Wen, Y.H. Luo, A.H. Liang and Z.L. Jiang, Sci Rep, 2014, 4, 3990.

[25] Y.G. Wu, S.S. Zhan, L.R. Xu, W.W. Shi, T. Xi, X.J. Zhan and P. Zhou, Chem Commun (Camb), 2011, 47, 6027.

[26] G. Frens, Nature, 1973, 241, 20.

[27] X.H. Ji, X.N. Song, J. Li, Y.B. Bai, W.S. Yang and X.G. Peng, J Am Chem Soc, 2007, 129, 13939.

[28] X.P. Jia, M.L. Xu, Y.Z. Wang, D. Ran, S. Yang and M. Zhang, Analyst, 2013, 138, 651.

[29] A. Davis and T. Tran, Hydrometallurgy, 1991, 26, 163.

[30] T.N. Angelidis, K.A. Kydros and K.A. Matis, Hydrometallurgy, 1993, 32, 143.

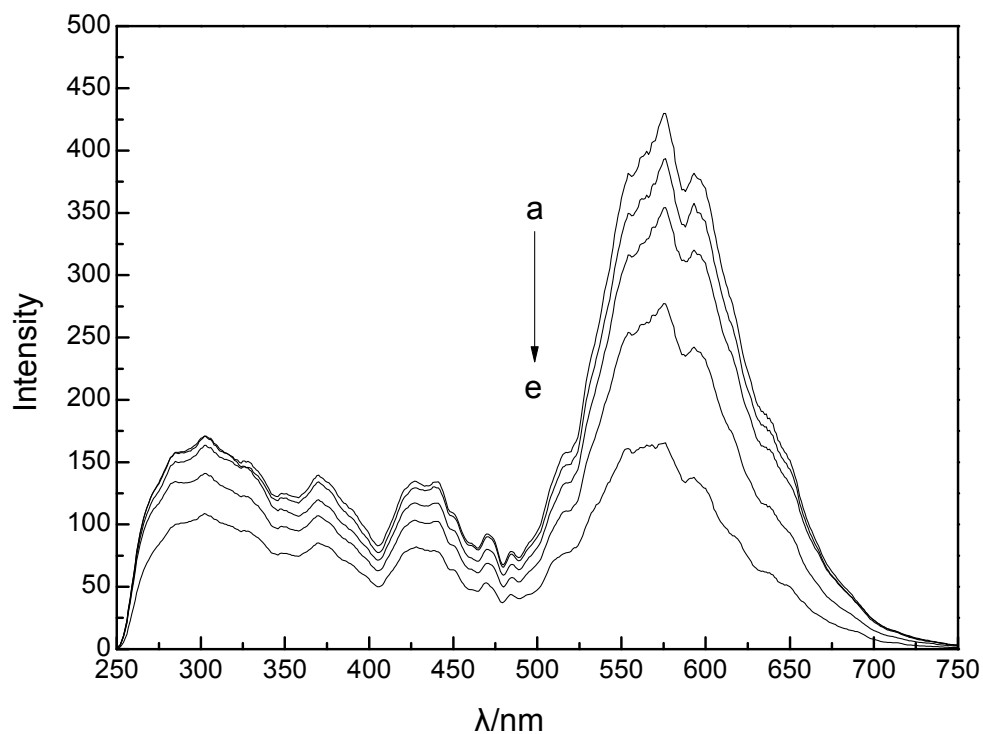[31] Z.Q. Zhang, H.W. Li, F. Zhang, Y.H. Wu, Z. Guo, L.Q. Zhou and J.D. Li, Langmuir, 2014, 30, 2648.

Fig. 1 Resonance light scattering spectra. a. pH 5.5 citric acid-trisodium citrate-KI-Hb-AuNPs; b. pH 5.5 citric acid-trisodium citrate-KI-AuNPs-3.24×10^{-6} mol/L H_2O_2; c. a-3.24×10^{-6} mol/L H_2O_2; d. a-6.48×10^{-6} mol/L H_2O_2; and e. a-1.296×10^{-5} mol/L H_2O_2. The concentrations of AuNPs, KI and Hb were 5.80 μg/mL, 6.0×10^{-3} mol/L, and 4.96×10^{-7} mol/L, respectively.
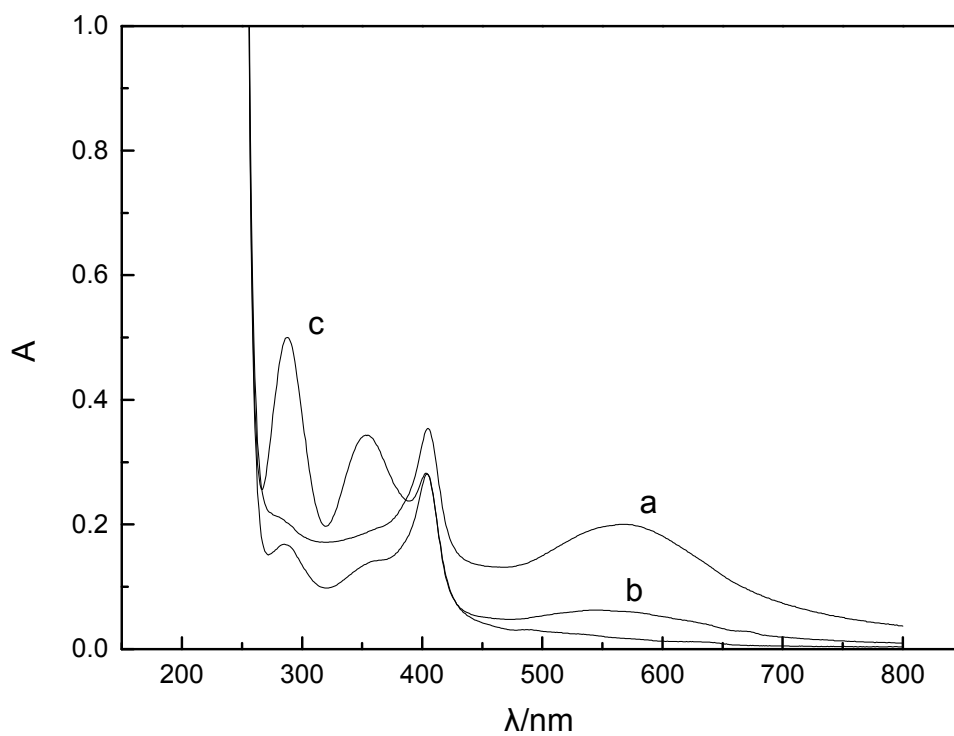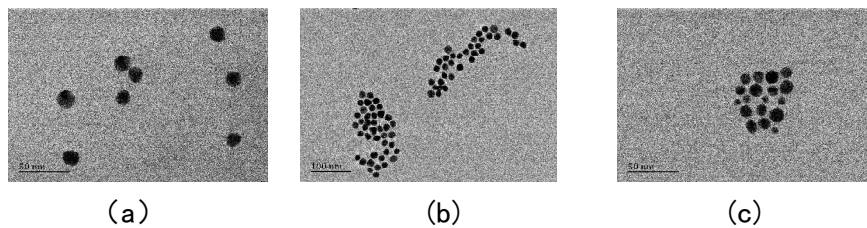
Fig. 2 Absorption spectra of different mixtures. a. pH 5.5 citric acid-trisodium citrate-KI-Hb-AuNPs; b. a-3.24×10^{-5} mol/L H$_2$O$_2$; and c. a-6.48×10^{-5} mol/L H$_2$O$_2$. The concentrations of AuNPs, KI and Hb were 5.80 μg/mL, 6.0×10^{-3} mol/L, and 4.96×10^{-7} mol/L, respectively.
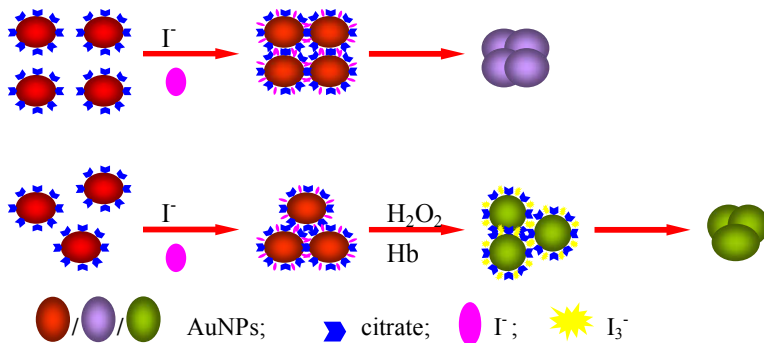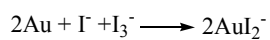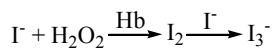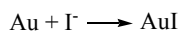
（a）   (b)   (c)

Fig. 3 Transmission electron microscopy images. a. AuNPs; b. pH 5.5 citric acid-trisodium citrate-KI-Hb-AuNPs; and c. b-6.48×10^{-6} mol/L H_2O_2. The concentrations of AuNPs, KI and Hb were 5.80 µg/mL, 6.0×10^{-3} mol/L, and 4.96×10^{-7} mol/L, respectively.

17

$$Au + I^- \longrightarrow AuI$$

$$I^- + H_2O_2 \xrightarrow{Hb} I_2 \xrightarrow{I^-} I_3^-$$

$$2Au + I^- + I_3^- \longrightarrow 2AuI_2^-$$

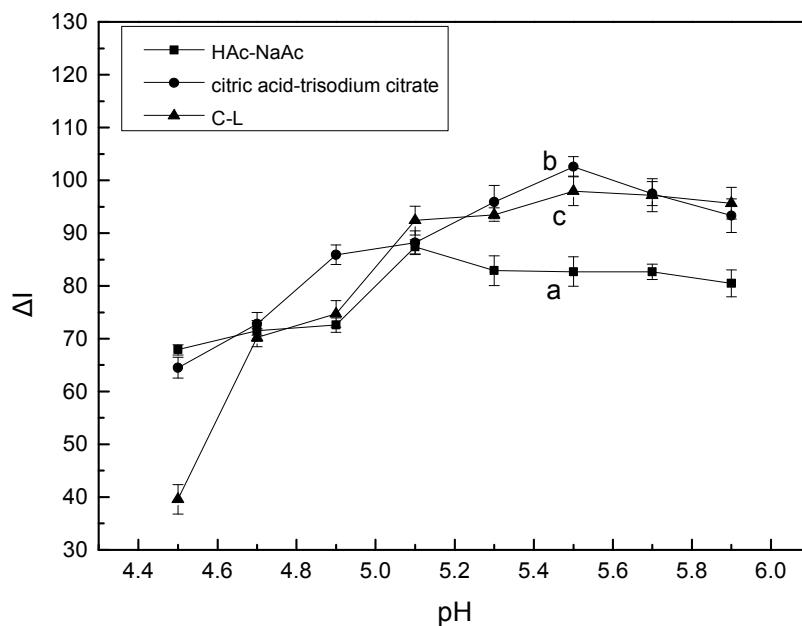Scheme 1 Schematic illustration of H_2O_2 detection using AuNPs and iodide.

Fig. 4 Effect of the buffer solution. a. HAc-NaAc-KI-Hb-AuNPs-H_2O_2; b. citric acid-trisodium citrate-KI-Hb-AuNPs-H_2O_2; and c.C-L-KI-Hb-AuNPs-H_2O_2. The concentrations of AuNPs, KI, Hb and H_2O_2 were 5.80 µg/mL, 6.0×10^{-3} mol/L, 4.96×10^{-7} mol/L, and 6.48×10^{-6} mol/L, respectively
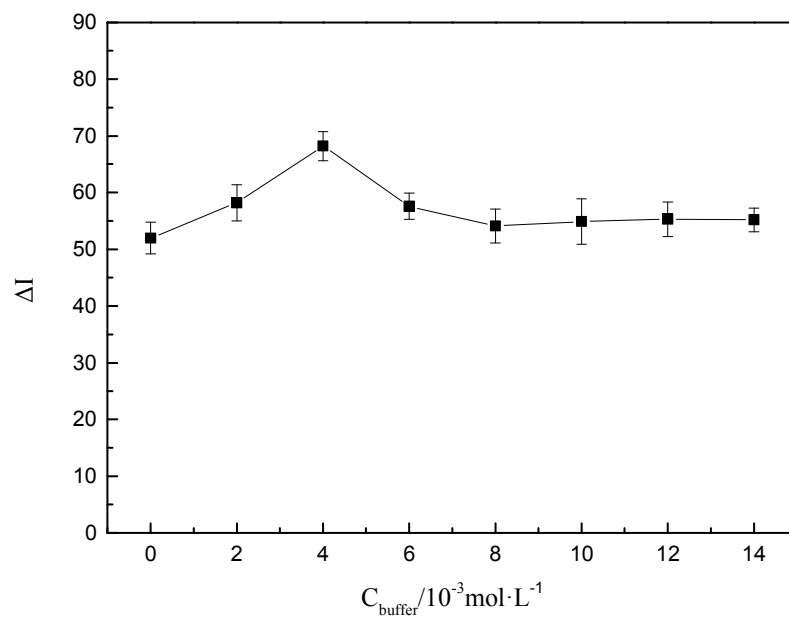
19

Fig. 5 Effect of the citric acid-trisodium citrate concentration on the ΔI response of the citric acid-trisodium citrate-Hb-KI-AuNPs system in the presence of 6.48×10^{-6} mol/L H_2O_2.

20

Fig. 6 Effect of the KI concentration on the ΔI response of the citric acid-trisodium citrate-Hb-KI-AuNPs system in the presence of 6.48×10^{-6} mol/L H_2O_2.
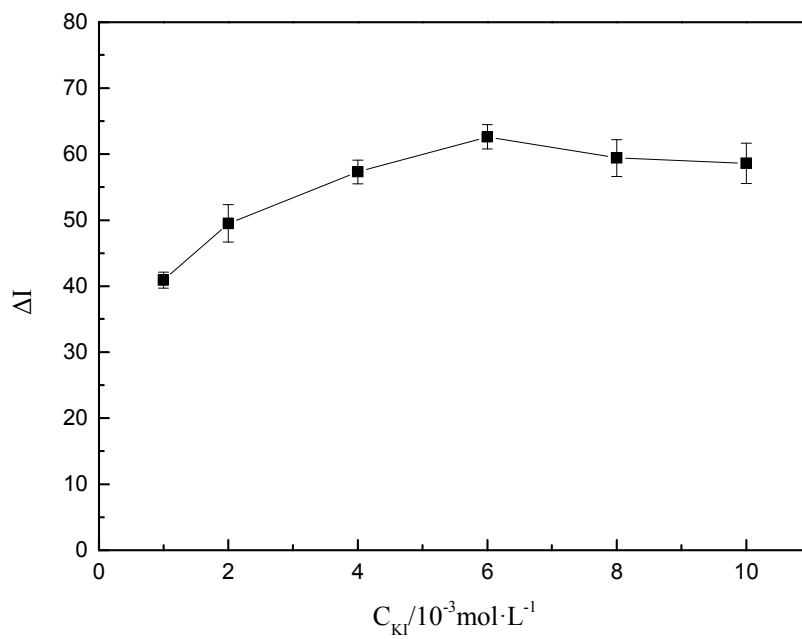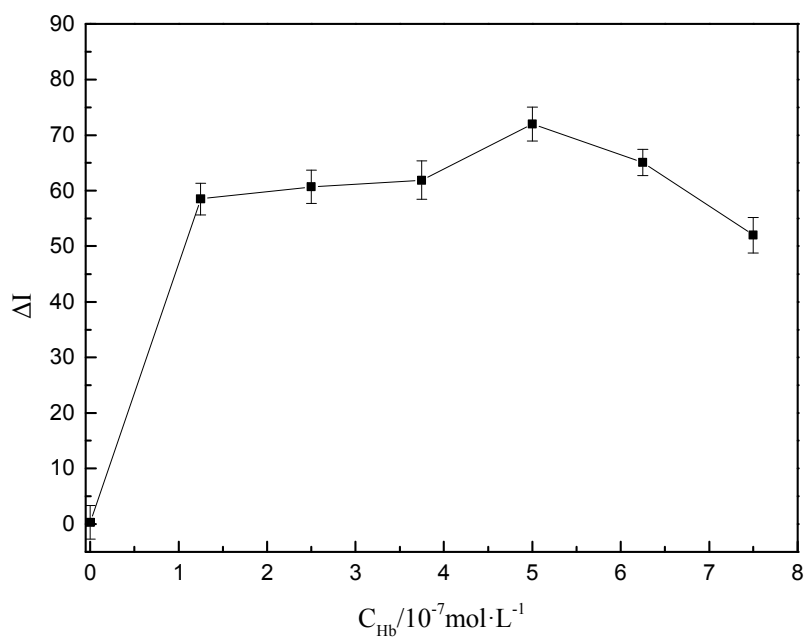
Fig. 7 Effect of the Hb concentration on the ΔI response of the citric acid-trisodium citrate-Hb-KI-AuNPs system in the presence of 6.48×10^{-6} mol/L H_2O_2.
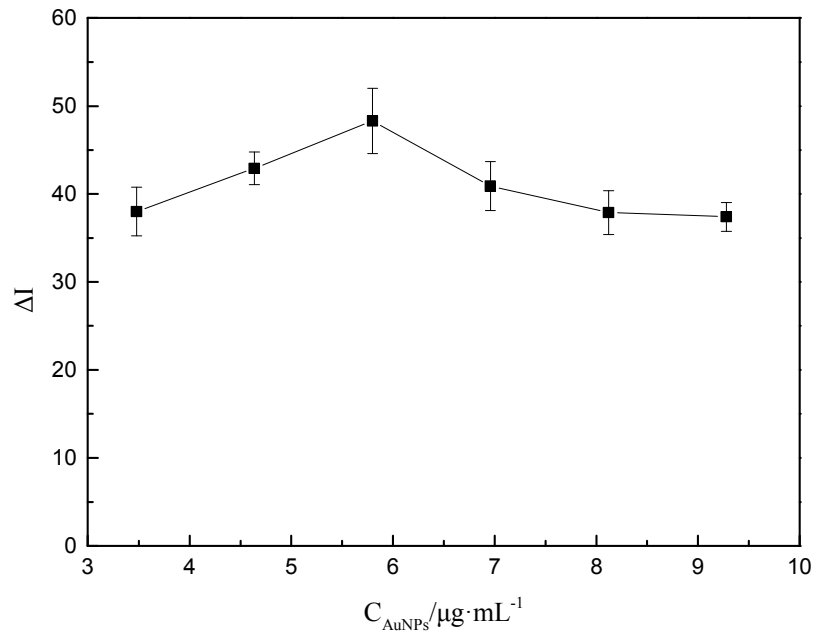
Fig. 8 Effect of the gold nanoparticle concentration on the ΔI response of the citric acid-trisodium citrate-Hb-KI-AuNPs system in the presence of 6.48×10^{-6} mol/L H_2O_2.

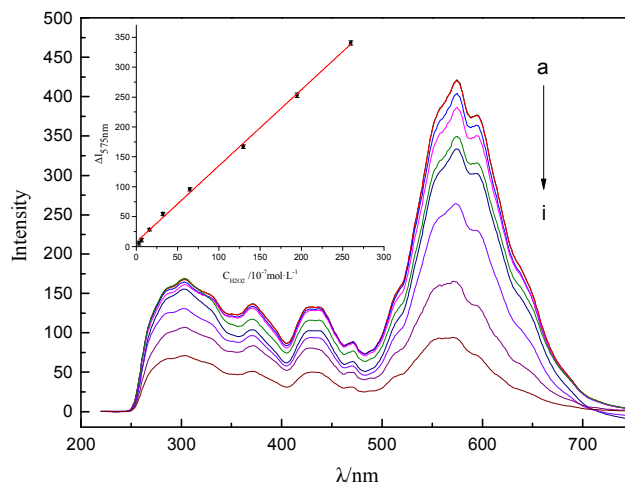Fig. 9 Resonance light scattering spectra of the KI-AuNPs system containing various concentrations of H_2O_2 (from top to bottom, (0, 3.248, 6.496, 16.24, 32.48, 64.96, 129.92, 194.88, 259.84) $\times 10^{-7}$ mol/L). The inset shows the linear calibration curve. Reaction conditions: pH=5.5; AuNP, KI and Hb concentrations of 5.80 μg/mL, 6.0×10^{-3} mol/L, and 4.96×10^{-7} mol/L, respectively.

1
2
3
4
5
6
7
8
9
10
11
12
13
14
15
16
17
18
19
20
21
22
23
24
25
26
27
28
29
30
31
32
33
34
35
36
37
38
39
40
41
42
43
44
45
46
47
48
49
50
51
52
53
54
55
56
57
58
59
60

Table 1 Comparison of some assays for H_2O_2.

Methods	Linear range	DL	Reference
Electrochemistry	0.5-970 μmol/L	0.1 μmol/L	[5]
Atomic absorption spectrometry	2.64-42.24 μmol/L	0.81 μmol/L	[9]
High performance liquid	15-300 μmol/L (HPLC-FD)	6 μmol/L	[11]
chromatography	7.4-15000 μmol/L (HPLC-ED)	0.6 μmol/L	[11]
Chemiluminescence	20-1600 μg/L	9 μg/L	[13]
Flow-injection analysis	1-100 μmol/L	0.29 μmol/L	[15]
Fluorescence	0-300 μmol/L	0.8 μmol/L	[16]
Nuclear magnetic resonance		20 μmol/L	[20]
Resonance light scattering	0.325-26 μmol/L	0.248 μmol/L	This paper

25

Table 2 Effect of foreign substances (6.48×10^{-6} mol/L H_2O_2).

Coexisting substance	Tolerance (μg/mL)	Relative error Er (%)	Coexisting substance	Tolerance (μg/mL)	Relative error Er (%)
Na^+, Cl^-	580	4.4	NO_3^-, Na^+	400	4.9
Zn^{2+}, Cl^-	5	4.8	SO_4^{2-}, K^+	160	4.6
Mg^{2+}, Cl^-	5	4.8	CO_3^{2-}, Na^+	2	4.9
Ca^{2+}, Cl^-	4	4.7	sucrose	262	4.6
Fe^{3+}, Cl^-	2	5.0	glucose	115	-4.8
Al^{3+}, Cl^-	2	3.8	taurine	20	5.0
L-proline	4	-4.1	DL-alanine	2	4.8
L-arginine	1	4.9	Vitamin C	2	3.6
K^+, H_2PO_4	45	3.2	Fe^{2+}, SO_4^{2-}	1	2.7
Vitamin A	1	4.3	Vitamin D	1	4.8
Vitamin E	2	4.4	Vitamin B_1	2	4.7
Vitamin B_2	2	4.5			

26

Table 3   Analytical results for H_2O_2 in milk samples (n=5).

Sample	Found (μmol/L)	Added (μmol/L)	Total found (μmol/L)	RSD (%)	Recovery (%)
Milk (Mengniu)	Not detected	6.48	6.04	3.4	93.2
		12.96	13.00	3.2	100.3
Milk (Yili)	Not detected	6.48	5.98	4.1	92.3
		12.96	12.57	3.9	97.0